Interactions between trans-resveratrol and CpLIP2 lipase/acyltransferase: Evidenced by fluorescence and in silico

Thi-Nga Nguyen, Eric E. Dubreucq, Véronique Perrier, Quang-Hung Tran, Claudine Charpentier, Clarence Charnay, Ferial Terki, Christian Jay-Allemand, Luc P.R. Bidel

Interactions between *trans*-resveratrol and CpLIP2 lipase/acyltransferase: Evidenced by fluorescence and *in silico*

Thi-Nga Nguyen[a,b,c], Eric Dubreucq[a], Veronique Perrier[a], Quang-Hung Tran[d],
Claudine Charpentier[a], Clarence Charnay[b], Ferial Terki[f], Christian Jay-Allemand[a],
Luc P.R. Bidel[e,*]

[a] UMR IATE, University of Montpellier, Montpellier SupAgro, INRAE, CIRAD, F-34060 Montpellier, France
[b] Institut Charles Gerhardt UMR 5253 CNRS-UM, University of Montpellier, F-34095 Montpellier, France
[c] Institute of Natural Products Chemistry, Vietnam Academy of Science and Technology, 18 Hoang Quoc Viet, 10000 Hanoi, Vietnam
[d] R&D&C, eV-Technologies, F-14000 Caen, France
[e] UMR AGAP, University of Montpellier, CIRAD, INRAE, Montpellier SupAgro, F-34060 Montpellier, France
[f] PhysMedExp, UMR CNRS 9214 – Inserm U1046, CHU Montpellier, University of Montpellier, France

ABSTRACT

We have examined the *trans*-resveratrol/lipase interaction by quantitative and qualitative analyses of fluorescence spectra, molecular docking and quantum-chemical calculations at DFT level. Interactions of CpLIP2 from *C. parapsilosis* CBS 604 and *trans*-resveratrol were confirmed with a major contribution of tryptophan residues to fluorescence quenching. A thermodynamic study across a wide temperature range was consistent with the presence of a single binding site with a binding free energy of -24 kJ/mol. Nevertheless, *trans*-resveratrol competitively inhibited CpLIP2 activity. Molecular docking and quantum-chemical calculations were consistent with a strong binding of *trans*-resveratrol to the CpLIP2 catalytic site via electrostatic and hydrophobic forces. The structural analysis quantitatively revealed an energy transfer from W51 and W350 to *trans*-resveratrol with a distance of 32 Å. Precise understanding of *trans*-resveratrol/CpLIP2 interactions has important implications on lipases for screening of stilbenoid.

1. Introduction

Trans-resveratrol, a polyphenol of the stilbene class is found in many fruits, has been studied extensively over decades. This natural agent exhibits many biological activities such as anticancer, antioxidant, anti-inflammatory, and cardioprotective properties (Berman, Motechin, Wiesenfeld, & Holz, 2017; Hsieh & Wu, 2010; Jang et al., 1997). Many targets of *trans*-resveratrol have been studied using *in vitro*, *in vivo*, and clinical trials. At the cellular level, *trans*-resveratrol has been revealed some effects on a variety of cells by inhibiting the activity of enzymes such as lipoxygenase, aromatase, 6-phosphofructo-1-kinase, and protein kinase D (Gomez et al., 2013; Haworth & Avkiran, 2001; Pinto, García-Barrado, & Macías, 1999).

The natural function of lipases (EC 3.1.1.3) is to catalyze the hydrolysis of esters of fatty acids. They are produced by bacteria, fungi, plants, and animals, and can be used in the textile, oleo-chemical, paper and food industries, as well as medical applications (Abhishek & Mukhopadhyay, 2012). A lipolytic activity has been shown to be a factor involved in the virulence and the pathogenicity of some fungi and bacteria (Gaillardin, 2010). *Candida parapsilosis* is one of the *Candida* species that causes of fungemia. Two putative lipase genes have been identified in *C. parapsilosis* CBS 604, but only, one of them, *CpLIP2*, codes for an active protein, with lipase/acyltransferase activity (Trofa, Gacser, & Nosanchuk, 2008). CpLIP2 shares homology with lipases from the related pathogenic yeast *C. albicans* (Hube et al., 2000; Neugnot, Moulin, Dubreucq, & Bigey, 2002). Secreted lipase activity has been demonstrated to be involved in the mechanism of infection by some *C. parapsilosis* and *C. albicans* strains (Gácser, Trofa, Schäfer, & Nosanchuk, 2007; Trofa et al., 2011).

Although previous studies have concerned the interaction between *trans*-resveratrol and albumins, nothing has been documented about its interaction with CpLIP2. Here, we have explored the *trans*-resveratrol/lipase interaction in aqueous medium by analyses of emission fluorescence spectra. This approach requires smaller amount of lipase compared to Isothermal Titration Calorimetry (ITC). It is highly sensitive for being carried out on native protein at low concentration within

---

* Corresponding author.
  E-mail address: luc.bidel@inrae.fr (L.P.R. Bidel).

physiological buffer and during short period, both preventing its aggregation. Working with fluorescence at low protein concentration also allow to study complexation of the poorly water soluble resveratrol. It also permits to avoid the potential artefacts of molecular immobilisation necessary for Surface Plasmon Resonance (SPR) and their associated limitations reported by Quinn *et al.* (Quinn (2012). We then described the enzymatic kinetics of CpLIP2 with *trans*-resveratrol as an inhibitor. Molecular docking and quantum-chemical calculations at the DFT level were performed to support the analysis of the interaction and inhibition. Understanding the interaction between *trans*-resveratrol and CpLIP2 could support to develop the screening of efficient stilbenes for target proteins.

2. Materials and methods

2.1. Chemicals and instruments

Recombinant CpLIP2 was produced by heterologous expression in *Komagataella* (*Pichia*) *pastoris* as described in Brunel et al. (2004).

Trans-resveratrol > 99% was purchased from Tokyo Chemical Industry Co. Ltd (W3ZZH-MQ, TCI Europe). Other chemicals were from Sigma-Aldrich unless otherwise specified. Aqueous solutions were prepared using ultrapure water (Milli-Q, Synergy Merk Millipore, Germany). The pH values were measured by a pH meter model WTW 313 (Weilheim, Germany). Absorbance spectra were recorded by a UV–Vis Jasco 650 spectrophotometer (Jasco, Japan), using a pair of matched 10-mm pathlength *Suprasil* quartz cuvettes. Emission and synchronous fluorescence spectra were carried out on an Edinburgh FS920 fluorescence spectrometer (Edinburgh Instruments, UK) in a controlled temperature room at 20 °C. The thermodynamic study was carried out with a thermostated quart cuvette using a Cary Eclipse fluorescence spectrometer (Varian, Australia). Fluorescence measurement used quartz cuvettes (101-QS, Hellma, Germany). Enzymatic kinetics were carried out in 96 wells UV-Star μClear microplates (Greiner-Bio-One, Germany) using an Enspire microplate reader (PerkinElmer, Singapore).

2.2. Interaction study

Lyophilized recombinant CpLIP2 and *trans*-resveratrol were dissolved in 50 mM TRIS-HCl, pH 6.5 buffer solution and stored at +3 °C. Stock solutions of CpLIP2 (2 μM) and *trans*-resveratrol (0–45 μM) in buffer at pH 6.5 were incubated for 1 h. Emission spectra were scanned from 285 nm to 500 nm with an excitation wavelength of 280 nm. Synchronous spectra were measured by keeping the deviation between excitation and emission monochromators ($\Delta\lambda = \lambda_{emission} - \lambda_{excitation}$) at 15 nm and 60 nm. See S1 for the correction method of fluorescence intensity.

2.3. Inhibition study

Since *trans*-resveratrol is poorly soluble in aqueous media (13.6 μg/g in pH 7.4 buffer (Hung, Fang, Liao, & Fang, 2007)), it was dissolved in absolute ethanol, and then mixed to buffer to obtain 1.6% (v/v) ethanol in the final mixture. Each microtube contained 2 μM–10 μM 4-methylumbelliferyl acetate (4-MuAc), 0.05 μM CpLIP2 and *trans*-resveratrol used at different concentrations of 0, 1.67, 6.67, 13.34 (μM). The fluorescence emission spectra were recorded at 440 nm ($\lambda_{excitation}$ = 310 nm) at 90 s intervals. The fluorescent intensity is corrected as detailed in S1.

2.4. Computational methods

The 3D structure of CpLIP2 lipase/acyltransferase (Subileau et al., 2015) protonated for pH 6.5 using PROPKA (Olsson, Søndergaard, Rostkowski, & Jensen, 2011), was minimized (2000 steps) then

equilibrated at 303 K during a 5 ns simulation using NAMD v2.13 (Phillips et al., 2005) with the QwikMD setup (Ribeiro et al., 2016), using the CHARMM36 protein force field (Best et al., 2012) in a periodic explicit solvent cubic box (edge length equal to the diagonal length of CpLIP2 plus 15 Å) filled with the TIP3P water model (Jorgensen, Chandrasekhar, Madura, Impey, & Klein, 1983), including an explicit NaCl concentration of 0.15 M, using a non-bonded forces cut off at 12 Å and with long-range electrostatics calculated using the Particle-Mesh-Ewald model. The initial geometry of *trans*-resveratrol was optimized using the ADF module of AMS 2018 (SCM, Amsterdam, NL) based on the density functional theory (DFT), using the PBE-D3(BJ) GGA functional with D3 dispersion correction and Becke-Johnson damping (Grimme, Ehrlich, & Goerigk, 2011), the TZ2P triple ζ basis set with double polarization using a small frozen core, and the COSMO (Klamt & Schuurmann, 1993) water solvation model.

Molecular docking was performed with Autodock Vina v1.1.2 (Trott & Olson, 2011) using the UCSF Chimera v1.13.1 (Pettersen et al., 2004) interface. The energy of the structures corresponding to the two poses with the highest Autodock score was minimized within Chimera with default parameters using the AMBER ff14SB and the AM1-SCC force fields for atomic partial charge calculations in the protein and the ligand, respectively, with the protein backbone constrained to fixed positions. The conformation with the lowest estimated energy was then selected for each ligand for further calculations. Diagrams of the main ligand-enzyme interactions were obtained using PoseView v1.1.2 (Biosolvit, Hamburg, DE). For each ligand, the geometry of the complex with the protein binding site was further optimized as follows to allow interaction energy calculations by DFT. First, sub-models restricted to the binding site were extracted by selecting all the residues with at least one atom closer than 5 Å from the bound resveratrol. The broken amide bonds of the protein backbone were restored by capping with –CO-CH$_3$ and –NH-CH$_3$ groups on the amino and carboxyl sides, respectively, aligned with the backbone of the neighboring residues. The sub-models obtained comprised about 450 atoms. Their geometry was then refined using the PM7 semi-empirical quantum chemical method and the COSMO water solvation model implemented in MOPAC 2016 (Stewart Computational Chemistry, Colorado Springs, CO, USA), with the position of C and N atoms of the protein backbone constrained to fixed positions. The interaction energy between resveratrol and the protein binding site was then analyzed by the extended transition state – natural orbitals for chemical valence (ETS-NOCV) (Mitoraj, Michalak, & Ziegler, 2009) decomposition method using ADF with the dispersion-corrected BP86-D3(BJ) GGA exchange-correlation functional and the DZ double ζ basis set with a large frozen core. For each ligand isomer, the two closed-shell molecular fragments defined for the analysis were resveratrol and the protein part of the sub-model.

3. Results and discussion

3.1. Interaction study by fluorescence quenching

We have studied the interaction of CpLIP2 and *trans*-resveratrol by characterizing the fluorescence emission intensity (at $\lambda_{excitation}$ = 280 nm) of CpLIP2 in the presence of different *trans*-resveratrol concentrations (Fig. 1A).

Two important pieces of information confirmed the interaction between CpLIP2 and *trans*-resveratrol: (*i*) The fluorescence quenching rate is proportional to the *trans*-resveratrol concentrations in the range from 0 to 45 μM. (*ii*) There is a redshift for the emission maximum wavelength from 335 nm to 361 nm. The fluorescence was analyzed using the Stern-Volmer equation (Lakowicz, 2006):

$$\frac{F_o}{F} = 1 + k_q \tau_o [Q] = 1 + K_{sv} [Q] \tag{1}$$

where F_o and F are the corrected fluorescence of CpLIP2 without and with *trans*-resveratrol, respectively; k_q is the quenching rate constant-
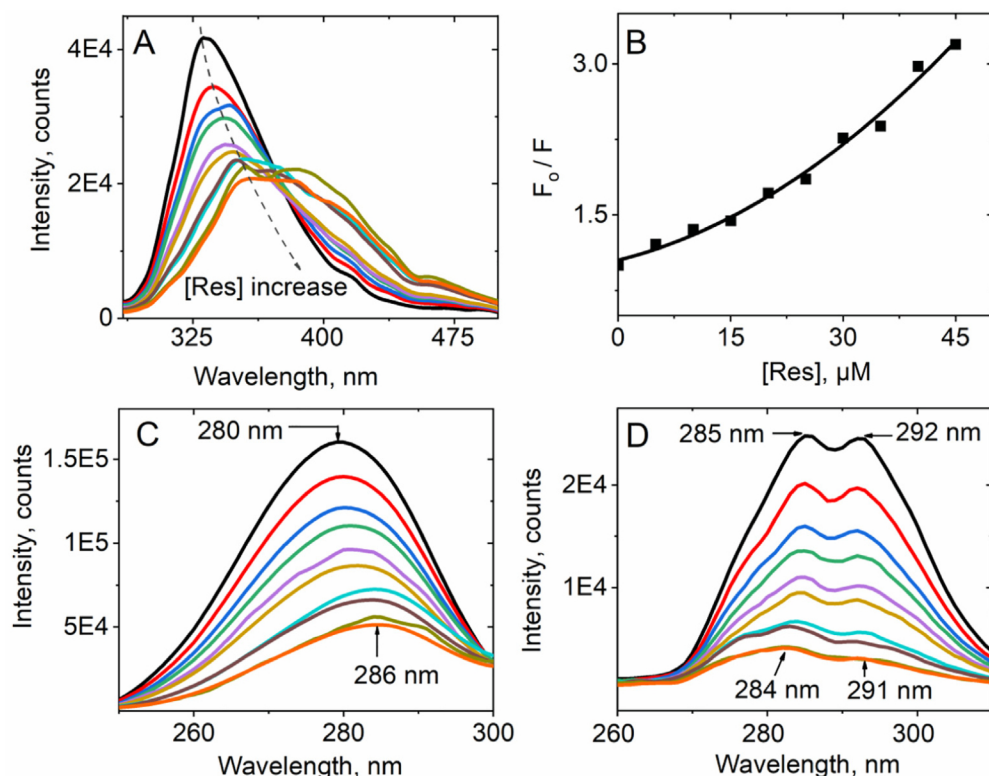
Fig. 1. (A) Fluorescence emission spectra of CpLIP2 (2 μM) with *trans*-resveratrol concentrations of 0, 5, 10, 15, 20, 25, 30, 35, 40, 45 (μM). The excitation wavelength was 280 nm; (B) Stern-Volmer plot of steady-state fluorescent intensity ratios of CpLIP2 in the absence (F_o) and in the presence of *trans*-resveratrol (F) as a function of *trans*-resveratrol concentration (solid squares). F_o and F values were selected at 335 nm from emission spectra. Synchronous spectra of CpLIP2 in solution with different *trans*-resveratrol concentrations at $\Delta\lambda = 60$ nm (C) and $\Delta\lambda = 15$ nm (D).

coefficient in solution; τ_o is the excited state time of CpLIP2 in the buffer; [Q] is *trans*-resveratrol concentration; K_{sv} is the association constant.

Many mechanisms involved in the interactions of proteins with their neighboring molecules result in a fluorescence quenching. Among them, there are excited-state interactions, molecular rearrangements, energy transfer, ground state complexation, and collisional quenching (Albani, 2007; Lakowicz, 2006). Dynamic quenching refers to collisional quenching, which occurs when the fluorophore encounters with quencher during the exciting lifetime. It facilitates the non-radiative transition pathway to the ground state. Static quenching occurs when the non-fluorescent complex is formed at the ground state. To understand the fluorescence quenching mechanism in this interaction set, we have analyzed the Stern-Volmer curve shown in Fig. 1B.

At low *trans*-resveratrol concentrations (0–20 μM), the response of F_o/F with *trans*-resveratrol concentrations could be considered as linear. However, the trend fits a second-order polynomial with a positive deviation from linearity when considering the whole range of concentrations (0–45 μM). Taking into account $\tau_o = 3.1$ ns as the average value usually employed for tryptophan residues, a K_{sv} value of 33,000 M^{-1} was obtained by fitting the Stern-Volmer equation to the linear part of the curve (0–20 μM *trans*-resveratrol). As a result, k_q was calculated to be about $1.1 \times 10^{13}\ M^{-1}\ s^{-1}$. This value is three orders of magnitude higher than the diffusion-limited quenching in water ($k_q = 10^{10}\ M^{-1}\ s^{-1}$), which confirms that the complex formation contributes significantly in the fluorescence quenching process (Acharya, Sanguansri, & Augustin, 2013; Ghisaidoobe & Chung, 2014). The positive deviation from the Stern-Volmer plot and the high k_q value indicate that the binding process of *trans*-resveratrol to CpLIP2 involves both the dynamic and the static quenching processes (Lakowicz, 2006). In addition to the reduction of fluorescence intensity observed in Fig. 1A, there is a redshift of the maximum emission wavelength from 335 nm (free CpLIP2) to 361 nm (the mixture of free CpLIP2 and CpLIP2-resveratrol complex). This redshift matches the well-known shift of the fluorescence emission peak of tryptophan to the maximum emission wavelength of unfolded proteins in an aqueous medium

(Havel, Kauffman, & Elzinga, 1988).

To evaluate the contribution of tryptophan and tyrosine residues to the protein fluorescence in the binding process, we have studied the synchronous spectra of tryptophan residues (Fig. 1C) and tyrosine residues (Fig. 1D) for CpLIP2 interacting with different *trans*-resveratrol concentrations. In these two measurement sets, the constant-wavelength difference ($\Delta\lambda$) between excitation and emission monochromators were set to 60 nm and 15 nm, respectively. We observed a decrease in the fluorescent intensity of both tryptophan and tyrosine residues with increasing *trans*-resveratrol concentrations. The fluorescence quenching of tryptophan was higher than tyrosine by about one order of magnitude, which indicated that interactions of *trans*-resveratrol and CpLIP2 seemed to result in strong conformation changes of some of the 7 tryptophan residues and a weak change for the 20 tyrosine residues. However, the average maximum peak of tryptophan residues shifted by 6 nm in the opposite direction to the blue shift of the average maximum peak of tyrosine residues, which was limited to about 1 nm. The redshift of the tryptophan maximum fluorescence wavelength indicated an increase of the polarity of the microenvironment of these residues. On the contrary, the blue shift of the tyrosine synchronous spectra was due to an increase in the hydrophobicity of tyrosine residues (Lakowicz, 2006). Interestingly, two fluorescence maxima at 292 nm and 284 nm were observed in the synchronous spectra associated with the tyrosine residues ($\Delta = 15$ nm). The maximum peak at 284 nm can be attributed to tyrosine residues whereas the maximum peak at 292 nm can be assigned to the tryptophan residues. This reveals an energy transfer from tyrosine to tryptophan, due to the overlap spectra between fluorescence emission of tyrosine and absorbance of tryptophan residues (Lakowicz, 2006).

3.2. Thermodynamics of trans-resveratrol – CpLIP2 interaction

To further study interactions between CpLIP2 and *trans*-resveratrol, we investigated the thermodynamic process through the fluorescence quenching (Fig. 2A) and the effect of temperature on the binding constant (Fig. 2B).
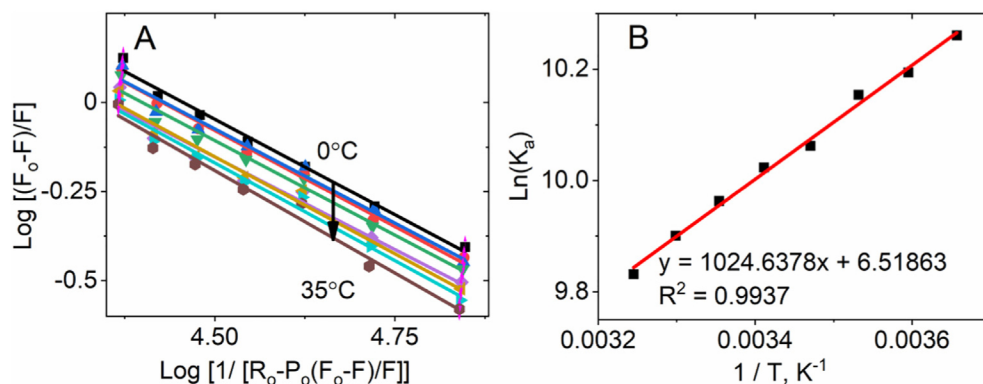
Fig. 2. (A) Plot of $Log[(F_o - F)/F]$ as a function of $Log[1/[R_o - P_o(F_o - F)/F]]$ for the binding of *trans*-resveratrol with CpLIP2 from 0 °C to 35 °C with 5 °C increment. The number of binding sites and the binding constant K_a were deduced by the slope and the intercept of the plots. (B) The Van't Hoff plot of $Ln(K_a)$ as a function of temperature. The variation of enthalpy and entropy were determined from the plot.

Eq. (2) was used to determine the number of binding sites and the binding constant of the interaction, as detailed by Shuyun Bi *et al.* (Bi et al. (2004).

$$Log\left(\frac{F_o - F}{F}\right) = -nLog\left(\frac{1}{R_o - P_o\left(\frac{F_o - F}{F}\right)}\right) + nLog(K_a) \quad (2)$$

where R_o and P_o are total *trans*-resveratrol and lipase concentration, n is a number of binding sites. K_a is the association constant, T is the absolute temperature (K) and R is ideal gas constant.

Fig. 2A plots the logarithm of $(F_o - F)/F$ *versus* the logarithm of $(1/[R_o - P_o(F_o - F)/F])$ in the temperature range from 0 to 35 °C. Fig. 2A shows the decrease of the fluorescence intensities when the temperature increases. From these plots and using Eq. (2), we deduced both binding site number (n) and binding constant (K_a) for each temperature (Table 1). We found that n values remained approximately 1 between 0 and 35 °C, whereas K_a decreased gradually with increasing temperature. It might reveal a change in lipase conformation.

When enthalpy change (ΔH) does not vary significantly in the eight investigated temperature values, both ΔH and entropy change (ΔS) can be determined from Van't Hoff equation based on the K_a values at different temperatures (Fig. 2B) [details are given in S2]. Under this hypothesis, ΔH and ΔS were calculated to be -8.5 kJ/mol and 54.19 J/mol, respectively.

Based on the contribution of ΔH and ΔS to the Gibbs energy (ΔG), stilbene binding to proteins can potentially be classified as Van der Waals force, electrostatic force, hydrogen bond and hydrophobic stacking of their aromatic rings to aromatic amino acid derivatives (Jakobek, 2015; Ozdal, Capanoglu, & Altay, 2013). With the calculated ΔH and ΔS values, Gibbs energies in the temperature range from 0 to 35 °C are determined to be negative values, varying from -23.3 kJ/mol to -25.2 kJ/mol as shown in Table 1. Therefore, the interactions in this temperature range are spontaneous.

The calculated ΔH and ΔS in this work are consistent with the published ones reported by Cao *et al.* (Cao, Wang, Tan, and Chen (2009), Jiang *et al.* (Jiang, Li, and Cao (2008) and Liu *et al.* (Liu, Shang,

Ren, and Li (2013). However, the inconsistencies were reported concerning the interpretation of these values. Cao *et al.* (Cao et al. (2009), and Jiang *et al.* (Jiang et al., 2008) stated that electrostatic forces were the major forces of the interaction. Liu *et al.* (Liu et al. (2013) relied on a relatively high value of ΔH compared to ΔS of about 1000 fold to confirm that hydrophobic interaction could be the main force involved in the interaction. In our work, quantum chemical calculations were also performed (Section 3.5) to decompose the contribution of charges and energies in the binding process between *trans*-resveratrol and CpLIP2, using the combined extended-transition-state energy decomposition analysis and natural orbitals for chemical valence (ETS-NOCV) method [26].

3.3. Förster resonance energy transfer (FRET) from CpLIP2 to trans-resveratrol.

According to the FRET theory (Lakowicz, 2006), the overlap region of CpLIP2 emission fluorescence spectrum and resveratrol absorbance spectrum (Fig. S1) corresponds to the energy transfer from a donor (CpLIP2) to an acceptor (*trans*-resveratrol). Förster distance R_o, the distance between CpLIP2 and *trans*-resveratrol r, and energy transfer efficiency E in the presence of CpLIP2 and different concentrations of *trans*-resveratrol were determined using Eqs. (S4)–(S7) in the Supplementary data S3 and given in Table S1.

The evaluated distances between two molecules (r) varied from 29 Å to 32 Å and r was comprised between $0.5R_o$ and $2R_o$ for all studied concentrations of *trans*-resveratrol. This was compatible with non-radiative energy transfer (Lakowicz, 2006; Poddubny & Rodina, 2016). The calculated energy transfer efficiency increased proportionally with *trans*-resveratrol concentrations. It is mainly due to the linear increment of the Förster distance R_o (from 24 Å to 36 Å) that is related to the increase of the overlap region (Fig. S1) between CpLIP2 emission fluorescence and *trans*-resveratrol absorbance spectrum. According to our results discussed in Fig. 1, the fluorescence quenching of CpLIP2 could be mainly due to tryptophan residues. So, the distances r are likely attributed to the distance between some tryptophan residues and *trans*-resveratrol molecules. To further understand the energy transfer from tryptophan (amongst W51, W177, W188, W294, W347, W350, W379) to *trans*-resveratrol, we extended this approach by molecular docking in the modeling Section 3.5.

3.4. Inhibition study

The inhibition kinetics of CpLIP2 by *trans*-resveratrol was studied using the Lineweaver-Burk equation deduced from the Michaelis-Menten model (Johnson & Goody, 2011; Lineweaver & Burk, 1934):

$$\frac{1}{V} = \frac{K_M}{V_{max}}\frac{1}{[S]} + \frac{1}{V_{max}} \quad (3)$$

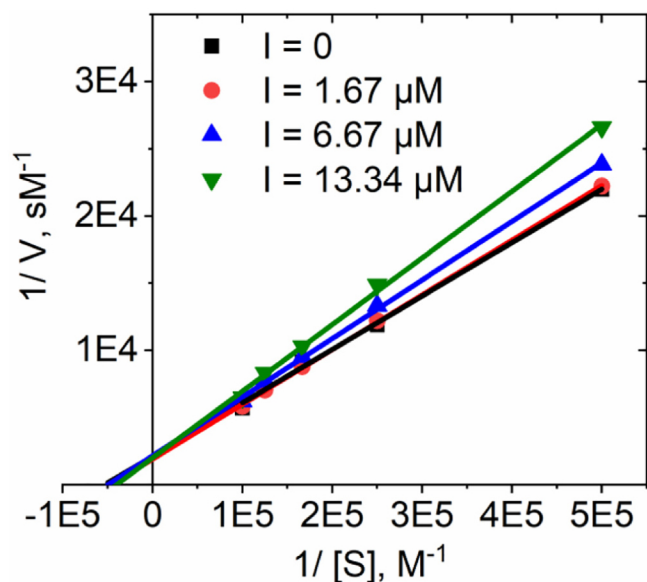where $[S]$ is the substrate concentration, V is the velocity of reaction,

Table 1
Binding parameters were calculated from 0 to 35 °C. ΔG was determined from enthalpy and entropy changes calculated to be -8.5 kJ/mol and 54.19 J/mol, respectively.

t, °C	n	K_a, M^{-1}	ΔG, kJ/mol	R^2
0	1.07	28.59×10^3	-23.31	0.987
5	1.08	26.75×10^3	-23.58	0.985
10	0.87	25.70×10^3	-23.85	0.972
15	0.86	23.44×10^3	-24.12	0.972
20	1.04	22.55×10^3	-24.39	0.957
25	0.90	21.23×10^3	-24.67	0.972
30	0.87	19.94×10^3	-24.94	0.979
35	0.86	18.61×10^3	-25.21	0.973

Fig. 3. Lineweaver-Burk plot of inverse reaction rate of CpLIP2 and substrate 4-MuAc as a function of inverse substrate concentration in the presence of inhibitor *trans*-resveratrol at various concentration. Substrate concentrations were 2, 4, 6, 8 and 10 μM; *trans*-resveratrol concentrations were 0, 1.67, 6.67 and 13.34 μM. The value of apparent V_{max} and K_M were given from the plot in Table 2.

V_{max} is the maximum rate of the reaction, K_M is the Michaelis constant.

To find the type of inhibition exerted by *trans*-resveratrol on CpLIP2, we have studied its effect on the kinetics of hydrolysis of the weak fluorescent substrate 4-methylumbelliferone acetate (4-MuAc) into the highly fluorescent product, 4-methylumbelliferone, at pH 7.0 and 30 °C. Fig. 3 shows the double reciprocal plot of the reaction rate as a function of 4-MuAc concentrations in the absence and presence of *trans*-resveratrol. The calculated results provided in Table 2 are compatible with a competitive inhibition model, with a constant value of V_{max} around 0.50 mM/s and a slight variation of K_M with *trans*-resveratrol concentration. This could indicate a competition of resveratrol with 4-MuAc at the same binding site.

3.5. Modeling

To support the analysis of the experimental results concerning a possible energy transfer between tryptophan residues and *trans*-resveratrol, a molecular docking study was performed using the CpLIP2 structure model (Subileau et al., 2015) equilibrated in a water box at 30 °C. *trans*-resveratrol was successfully docked in the active site of CpLIP2.

Fig. 4 shows the docking of *trans*-resveratrol in CpLIP2 after minimization of the complex structure in a water solvent box. Fig. 4A shows *trans*-resveratrol in the catalytic site of the lipase/acyltransferase. The total energy of the interaction was decomposed into London dispersion energy (hydrophobic interactions), orbital interactions and steric interactions (Fig. 4B). Two main hydrogen bonds between *trans*-resveratrol and backbone carbonyl groups of CpLIP2 binding site were found, representing 23% of total orbital interactions. Both hydrophobic and

electrostatic interactions significantly contributed to the total binding energy, accounting for 61% and 74% of the total binding energy. Steric interaction energy (+13.1 kcal/mol) was the sum of Pauli repulsion (+88.5 kcal/mol) and electrostatic interactions (−75.4 kcal/mol). Globally, the calculated binding energy was −102 kcal/mol.

It is noteworthy that when *trans*-resveratrol is dissolved in buffer at pH = 6.5 (experimental condition), a small fraction is isomerized into *cis*-resveratrol, and therefore, protein potentially interacts with both isomers. Structure modeling indicated that both isomers could indeed fit in the catalytic site of CpLIP2, and interact with different amino acid residues. However, *ab initio* interaction energy calculations performed on the minimized structures indicated a higher stabilization (by −14 kcal/mol) of the *trans*-resveratrol complex compared to *cis*-resveratrol (see Fig. S2).

The average distances between the center of the docked *trans*-resveratrol molecule and the 7 tryptophan residues in CpLIP2 are given in Table S2. Among them, W51, W294, and W350 are located at the protein surface, while the others are buried in the protein core. Their distances to the docked *trans*-resveratrol molecule were 31 Å, 23 Å and 32 Å, respectively, in fair agreement with the distance of 32 Å calculated above from experimental data (Fig. 4C and Table 1).

4. Conclusion

This study showed a spontaneous binding of *trans*-resveratrol with CpLIP2. The binding strongly quenched the fluorescence resulting from a population of 7 tryptophan residues in the protein and induced a fluorescence redshift, whereas it weakly quenched fluorescence resulting from the population of 20 tyrosine residues. Hydrophobic and electrostatic forces have been identified as major components, of similar importance, in the binding interactions according to thermodynamic parameters deduced from the fluorescence study and from quantum-chemical calculations based on a structural interaction model. A study of the inhibition of CpLIP2 hydrolytic activity revealed a competitive inhibition by *trans*-resveratrol in our assay conditions. Molecular docking simulations confirmed a possible binding of this molecule in the enzyme catalytic pocket. These arguments are consistent with the access of *trans*-resveratrol to the catalytic site of CpLIP2, explaining its competitive behavior with 4-MuAc substrate, and suggest that *trans*-resveratrol may also compete with the lipid substrates targeted by the lipases during infections by *C. parapsilosis*. Based on the close structural homology between CpLIP2 and some lipases from the related pathogen yeast *C. albicans*, these results may also have implications for other fungi. In this paper, the fluorescence study is an alternative approach to obtain the thermodynamic parameters of steady-state affinity and the kinetic binding constants (K_{in} and K_{out}) of the complexation, which could be achieved by the ITC or Microscale Thermophoresis (MST) and surface Plasmon Resonance (SPR) measurements, respectively.

Credit authorship contribution statement

Thi-Nga Nguyen: Investigation, Writing - Original draft. **Eric Dubreucq:** Methodology, and Software of simulation, Writing – Review & Editing manuscript. **Veronique Perrier:** Resource for CpLIP2 lipase production. **Quang-Hung Tran, Ferial Terki, and Christian Jay-Allemand:** Review and Editing the manuscript, Funding acquisition. **Claudine Charpentier, and Clarence Charnay:** Resource for the instruments, materials. **Luc P.R. Bidel:** Methodology, Conceptualization, Validation, Supervision.

Declaration of Competing Interest

The authors declare that they have no known competing financial interests or personal relationships that could have appeared to influence the work reported in this paper.

Table 2
Apparent V_{max} and K_M value deduced from the Lineweaver-Burk equation.

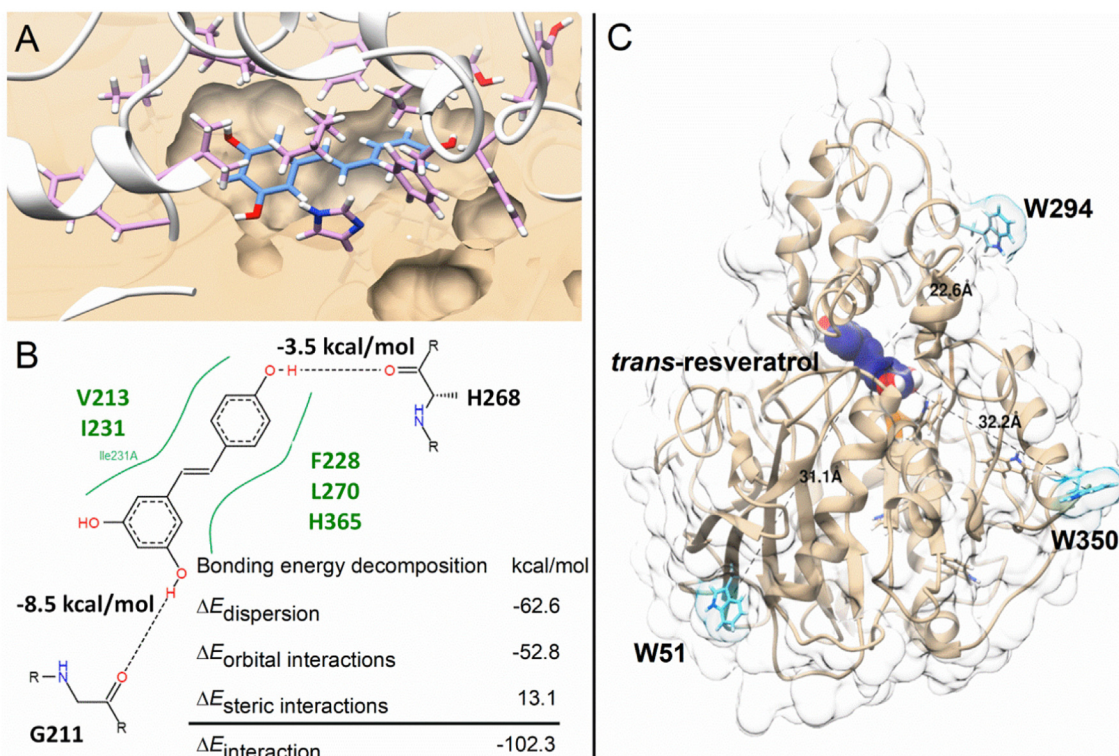| [Res], M	V_{max}, M/s	K_M, M	R^2
0	0.00047	1.9×10^{-5}	0.997
1.67×10^{-6}	0.00052	2.1×10^{-5}	0.999
6.67×10^{-6}	0.00046	2.0×10^{-5}	0.998
13.34×10^{-6}	0.00049	2.5×10^{-5}	0.997

Fig. 4. (A) *trans*-resveratrol, in blue, bound to CpLIP2. Residues with at least 1 atom closer than 5 Å from *trans*-resveratrol are shown in pink. The protein molecular surface is clipped to show the binding pocket. Some ribbons in front of the image have been hidden for clarity. (B) Scheme of the main interactions of *trans*-resveratrol with CpLIP2 active site residues based on the minimized geometry of the complex. ETS-NOCV energy decomposition was calculated at the BP86-D3(BJ)/DZ level of the density functional theory. Dotted lines: hydrogen bonds; green lines: main hydrophobic interactions. (C) Distance between *trans*-resveratrol docked in the catalytic pocket of CpLIP2 and the three tryptophan residues exposed to solvent. (For interpretation of the references to colour in this figure legend, the reader is referred to the web version of this article.)

Acknowledgments

References

Abhishek, K. S., & Mukhopadhyay, M. (2012). Overview of fungal lipase: A review. *Applied Biochemistry and Biotechnology, 166*(2), 486–520. https://doi.org/10.1007/s12010-011-9444-3.

Acharya, D. P., Sanguansri, L., & Augustin, M. A. (2013). Binding of resveratrol with sodium caseinate in aqueous solutions. *Food Chemistry, 141*(2), 1050–1054. https://doi.org/10.1016/j.foodchem.2013.03.037.

Albani, J. R. (2007). *Principles and applications of fluorescence spectroscopy.* Blackwell Publishing.

Berman, A. Y., Motechin, R. A., Wiesenfeld, M. Y., & Holz, M. K. (2017). The therapeutic potential of resveratrol: A review of clinical trials. *NPJ Precision Oncology, 1*(July), 1–35. https://doi.org/10.1038/s41698-017-0038-6.

Best, R. B., Zhu, X., Shim, J., Lopes, P. E. M., Mittal, J., Feig, M., & Jr, A. D. M. (2012). Optimization of the additive CHARMM all-atom protein force field targeting improved sampling of the backbone φ, ψ and side- chain χ1 and χ2 dihedral angles. *Journal of Chemical Theory and Computation, 8*(9), 3257–3273. https://doi.org/10.1021/ct300400x.

Bi, S., Ding, L., Tian, Y., Song, D., Zhou, X., Liu, X., & Zhang, H. (2004). Investigation of the interaction between flavonoids and human serum albumin. *Journal of Molecular Structure, 703*(1–3), 37–45. https://doi.org/10.1016/j.molstruc.2004.05.026.

Brunel, L., Neugnot, V., Landucci, L., Boze, H., Moulin, G., Bigey, F., & Dubreucq, E. (2004). High-level expression of *Candida parapsilosis* lipase/acyltransferase in *Pichia pastoris*. *Journal of Biotechnology, 111*(1), 41–50. https://doi.org/10.1016/j.jbiotec.2004.03.007.

Cao, S., Wang, D., Tan, X., & Chen, J. (2009). Interaction between trans-resveratrol and Serum Albumin in aqueous solution. *Journal of Solution Chemistry, 38*(9), 1193–1202. https://doi.org/10.1007/s10953-009-9439-7.

Gácser, A., Trofa, D., Schäfer, W., & Nosanchuk, J. D. (2007). Targeted gene deletion in *Candida parapsilosis* demonstrates the role of secreted lipase in virulence. *Journal of Clinical Investigation, 117*(10), 3049–3058. https://doi.org/10.1172/JCI32294.

Gaillardin, C. (2010). Lipases as pathogenicity factors of fungi. In K. N. Timmis (Ed.). *Handbook of hydrocarbon and lipid microbiology* (pp. 3259–3268). Berlin, Heidelberg: Springer.

Ghisaidoobe, T. A. B., & Chung, S. J. (2014). Intrinsic tryptophan fluorescence in the detection and analysis of proteins: A focus on förster resonance energy transfer techniques. *International Journal of Molecular Sciences, 15*(12), 22518–22538. https://doi.org/10.3390/ijms151222518.

Gomez, L. S., Zancan, P., Marcondes, M. C., Ramos-Santos, L., Meyer-Fernandes, J. R., Sola-Penna, M., & Silva, D. Da. (2013). Resveratrol decreases breast cancer cell viability and glucose metabolism by inhibiting 6-phosphofructo-1-kinase. *Biochimie, 95*(6), 1336–1343. https://doi.org/10.1016/j.biochi.2013.02.013.

Grimme, S., Ehrlich, S., & Goerigk, L. (2011). Effect of the damping function in dispersion corrected density functional theory. *Journal of Computational Chemistry, 32*(7), 1456–1465. https://doi.org/10.1002/jcc.21759.

Havel, H. A., Kauffman, E. W., & Elzinga, P. A. (1988). Fluorescence quenching studies of bovine growth hormone in several conformational states. *Biochimica et Biophysica Acta, 955*(2), 154–163. https://doi.org/10.1016/0167-4838(88)90189-6.

Haworth, R. S., & Avkiran, M. (2001). Inhibition of protein kinase D by resveratrol. *Biochemical Pharmacology, 62*(12), 1647–1651. https://doi.org/10.1016/S0006-2952(01)00807-3.

Hsieh, T., & Wu, J. M. (2010). Resveratrol: Biological and pharmaceutical properties as anticancer molecule. *BioFactors, 36*(5), 360–369. https://doi.org/10.1002/biof.105.

Hube, B., Stehr, F., Bossenz, M., Mazur, A., Kretschmar, M., & Schafer, W. (2000). Secreted lipases of *Candida albicans*: Cloning, characterisation and expression analysis of a new gene family with at least ten members. *Archives of Microbiology, 174*(5), 362–374. https://doi.org/10.1007/s002030000218.

Hung, C.-F., Fang, C.-L., Liao, M.-H., & Fang, J.-Y. (2007). The effect of oil components on the physicochemical properties and drug delivery of emulsions: Tocol emulsion versus lipid emulsion. *International Journal of Pharmaceutics, 335*(1–2), 193–202. https://doi.org/10.1016/j.ijpharm.2006.11.016.

Jakobek, L. (2015). Interactions of polyphenols with carbohydrates, lipids and proteins. *Food Chemistry, 175*(May), 556–567. https://doi.org/10.1016/j.foodchem.2014.12.013.

Jang, M., Cai, L., Udeani, G. O., Slowing, K. V., Thomas, C. F., Beecher, C. W. W., ... Pezzuto, J. M. (1997). Cancer chemopreventive activity of resveratrol, a natural product derived from grapes. *Science, 275*(5297), 218–220. https://doi.org/10.1126/science.275.5297.218.

Jiang, X. Y., Li, W. X., & Cao, H. (2008). Study of the interaction between trans-resveratrol and BSA by the multi-spectroscopic method. *Journal of Solution Chemistry, 37*(11), 1609–1623. https://doi.org/10.1007/s10953-008-9323-x.

Johnson, K. A., & Goody, R. S. (2011). The kinetics of invertase action – Translation of the 1913 Michaelis-Menten paper. *Biochemistry, 50*(39), 8264–8269. https://doi.org/10.1021/bi201284u.

Jorgensen, W. L., Chandrasekhar, J., Madura, J. D., Impey, R. W., & Klein, M. L. (1983). Comparison of simple potential functions for simulating liquid water. *Journal of Chemical Physics, 79*(2), 926–935. https://doi.org/10.1063/1.445869.

Klamt, A., & Schuurmann, G. (1993). COSMO: A new approach to dielectric screening in solvents with explicit expressions for the screening energy and its gradient. *Journal of the Chemical Society, Perkin Transaction, 2, 0*(5), 799–805. https://doi.org/10.1039/P29930000799.

Lakowicz, Joseph R. (2006). Principles of fluorescence spectroscopy. *Principles of Fluorescence Spectroscopy*. https://doi.org/10.1007/978-0-387-46312-4.

Lineweaver, H., & Burk, D. (1934). The determination of enzyme dissociation constants. *Journal of the American Chemical Society, 56*(3), 658–666. https://doi.org/10.1021/ja01318a036.

Liu, X., Shang, Y., Ren, X., & Li, H. (2013). Molecular modeling and spectroscopic studies on the interaction of transresveratrol with Bovine Serum Albumin. *Journal of Chemistry, 2013*, 1–7. https://doi.org/10.1155/2013/494706.

Mitoraj, M. P., Michalak, A., & Ziegler, T. (2009). A combined charge and energy decomposition scheme for bond analysis. *Journal of Chemical Theory and Computation, 5*(4), 962–975. https://doi.org/10.1021/ct800503d.

Neugnot, V., Moulin, G., Dubreucq, E., & Bigey, F. (2002). The lipase/acyltransferase from *Candida parapsilosis. European Journal of Biochemistry, 269*(6), 1734–1745. https://doi.org/10.1046/j.1432-1327.2002.02828.x.

Olsson, M. H. M., Søndergaard, C. R., Rostkowski, M., & Jensen, J. H. (2011). PROPKA3: Consistent treatment of internal and surface residues in empirical pKa predictions. *Journal of Chemical Theory and Computation, 7*(2), 525–537. https://doi.org/10.1021/ct100578z.

Ozdal, T., Capanoglu, E., & Altay, F. (2013). A review on protein-phenolic interactions and associated changes. *Food Research International, 51*(2), 954–970. https://doi.org/10.1016/j.foodres.2013.02.009.

Pettersen, E. F., Goddard, T. D., Huang, C. C., Couch, G. S., Greenblatt, D. M., Meng, E. C., & Ferrin, T. E. (2004). UCSF Chimera—A visualization system for exploratory research and analysis. *Journal of Computational Chemistry, 25*(13), 1605–1612. https://doi.org/10.1002/jcc.20084.

Phillips, J. C., Braun, R., Wang, W., Gumbart, J., Tajkhorshid, E., Villa, E., ... Schulten, K. (2005). Scalable molecular dynamics with NAMD. *Journal of Computational Chemistry, 26*(16), 1781–1802. https://doi.org/10.1002/jcc.20289.

Pinto, M. C., García-Barrado, J. A., & Macías, P. (1999). Resveratrol is a potent inhibitor of the dioxygenase activity of lipoxygenase. *Journal of Agricultural and Food Chemistry, 47*(12), 4842–4846. https://doi.org/10.1021/jf990448n.

Poddubny, A. N., & Rodina, A. V. (2016). Nonradiative and radiative Förster energy transfer between quantum dots. *Journal of Experimental and Theoretical Physics, 122*(3), 531–538. https://doi.org/10.1134/S1063776116030092.

Quinn, J. G. (2012). Modeling Taylor dispersion injections: Determination of kinetic/affinity interaction constants and diffusion coefficients in label-free biosensing. *Analytical Biochemistry, 421*(2), 391–400. https://doi.org/10.1016/j.ab.2011.11.024.

Ribeiro, J. V., Bernardi, R. C., Rudack, T., Stone, J. E., Phillips, J. C., Freddolino, P. L., & Schulten, K. (2016). QwikMD – Integrative molecular dynamics toolkit for novices and experts. *Scientific Reports, 6*(May), 1–14. https://doi.org/10.1038/srep26536.

Subileau, M., Jan, A.-H., Nozac'h, H., Pérez-Gordo, M., Perrier, V., & Dubreucq, E. (2015). The 3D model of the lipase/acyltransferase from *Candida parapsilosis*, a tool for the elucidation of structural determinants in CAL-A lipase superfamily. *Biochimica et Biophysica Acta-Proteins and Proteomics, 1854*(10), 1400–1411. https://doi.org/10.1016/j.bbapap.2015.06.012.

Trofa, D., Gacser, A., & Nosanchuk, J. D. (2008). *Candida parapsilosis*, an emerging fungal pathogen. *Clinial Mcrobiology Reviews, 21*(4), 606–625. https://doi.org/10.1128/CMR.00013-08.

Trofa, D., Soghier, L., Long, C., Nosanchuk, J. D., Gacser, A., & Goldman, D. L. (2011). A rat model of neonatal candidiasis demonstrates the importance of lipases as virulence factors for *Candida albicans* and *Candida parapsilosis. Mycopathologia, 172*(3), 169–178. https://doi.org/10.1007/s11046-011-9429-3.

Trott, O., & Olson, A. J. (2011). AutoDock Vina: Improving the speed and accuracy of docking with a new scoring function, efficient optimization and multithreading. *Journal of Computational Chemistry, 31*(2), 455–461. https://doi.org/10.1002/jcc.21334.